A population of gut epithelial enterochromaffin cells is mechanosensitive and requires Piezo2 to convert force into serotonin release

Constanza Alcaino[a], Kaitlyn R. Knutson[a], Anthony J. Treichel[a], Gulcan Yildiz[a], Peter R. Strege[a], David R. Linden[a,b], Joyce H. Li[c], Andrew B. Leiter[c], Joseph H. Szurszewski[a,b], Gianrico Farrugia[a,b], and Arthur Beyder[a,b,1]

[a]Enteric Neuroscience Program, Division of Gastroenterology & Hepatology, Mayo Clinic, Rochester, MN 55905; [b]Department of Physiology & Biomedical Engineering, Mayo Clinic, Rochester, MN 55905; and [c]Division of Gastroenterology, Department of Medicine, University of Massachusetts Medical School, Worcester, MA 01655

Edited by Ardem Patapoutian, The Scripps Research Institute, La Jolla, CA, and approved June 28, 2018 (received for review March 22, 2018)

Enterochromaffin (EC) cells constitute the largest population of intestinal epithelial enteroendocrine (EE) cells. EC cells are proposed to be specialized mechanosensory cells that release serotonin in response to epithelial forces, and thereby regulate intestinal fluid secretion. However, it is unknown whether EE and EC cells are directly mechanosensitive, and if so, what the molecular mechanism of their mechanosensitivity is. Consequently, the role of EE and EC cells in gastrointestinal mechanobiology is unclear. Piezo2 mechanosensitive ion channels are important for some specialized epithelial mechanosensors, and they are expressed in mouse and human EC cells. Here, we use EC and EE cell lineage tracing in multiple mouse models to show that Piezo2 is expressed in a subset of murine EE and EC cells, and it is distributed near serotonin vesicles by superresolution microscopy. Mechanical stimulation of a subset of isolated EE cells leads to a rapid inward ionic current, which is diminished by Piezo2 knockdown and channel inhibitors. In these mechanosensitive EE cells force leads to Piezo2-dependent intracellular Ca^{2+} increase in isolated cells as well as in EE cells within intestinal organoids, and Piezo2-dependent mechanosensitive serotonin release in EC cells. Conditional knockout of intestinal epithelial Piezo2 results in a significant decrease in mechanically stimulated epithelial secretion. This study shows that a subset of primary EE and EC cells is mechanosensitive, uncovers Piezo2 as their primary mechanotransducer, defines the molecular mechanism of their mechanotransduction and mechanosensitive serotonin release, and establishes the role of epithelial Piezo2 mechanosensitive ion channels in regulation of intestinal physiology.

mechanosensitivity | ion channel | serotonin | gastrointestinal | enterochromaffin cell

Digestion is a critical function of the gastrointestinal (GI) tract. This process relies on coordinated fluid secretion and motility in response to luminal mechanical stimuli. Landmark studies showed that mechanical stimulation of GI mucosa leads to serotonin (5-hydroxytryptamine, 5-HT) release (1, 2), which stimulates fluid secretion (3, 4) and GI motility (5). The enterochromaffin (EC) cells constitute the largest population of epithelial enteroendocrine (EE) cells, and contain large quantities of serotonin (6, 7). Thus, the EC cells were proposed to serve as specialized epithelial mechanosensors (1, 8). Indeed, force leads to 5-HT release in immortalized neuroendocrine cell lines (9–11). However, it is not known whether primary EE and EC cells are mechanosensitive, so their roles in GI mechanobiology remain unclear.

The mechanosensitive ion channel Piezo2 is expressed in human and mouse EC cells (11). This is intriguing because EC cells are similar to Merkel cells, which are epithelial light-touch sensors of the skin that rely on Piezo2 for mechanotransduction (12, 13) and also release 5-HT (14). We wanted to test the hypothesis that EE cells, and specifically EC cells, are mechanosensitive and that EC cell Piezo2 channels control mechanically induced 5-HT release to regulate force-dependent epithelial secretion. Our results show that in murine small- and large-intestine epithelium, Piezo2 is expressed in a subset of EC cells, where it is localized in the membrane close to 5-HT vesicles. A lineage-traced mechanosensitive EE cell subset expresses both Piezo2 mRNA and protein, and requires Piezo2 for mechanosensitive ionic currents, intracellular Ca^{2+} increase, and EC cell 5-HT release. Conditional GI epithelium Piezo2 knockout significantly decreases pressure-induced epithelial secretion. Our results strongly suggest that the mechanosensitive ion channel Piezo2 is the primary EE cell mechanosensor, and that in EC cells it is critical for coupling force to 5-HT release and intestinal secretion.

Results

EC Cell Subset Specifically Expresses Piezo2. We used the *Tph1-CFP* mouse model to identify EC cells, as we did in a recent study (11). Tph-1 is the most specific marker of EC cells (15), because it is the enzyme required for 5-HT synthesis specifically in nonneuronal cells (7). We found that epithelial Piezo2 was expressed specifically in some but not all EC cells in both small (Fig. 1 *A–C*) and large (Fig. 1 *D–F*) intestine. We quantified Piezo2 distribution. We found that out of all epithelial $Piezo2^+$ cells, $Piezo2^+$ EC cells ($Tph1^+P2^+/P2^+$) made up 85 ± 7% in small and 81 ± 3% in large intestine. On the other hand, of all EC cells, $Piezo2^+$ EC cells ($Tph1^+P2^+/Tph1^+$) made up 69 ± 7%

Significance

Mechanical forces are important for normal gastrointestinal tract function. The enterochromaffin cells in the gastrointestinal epithelium have been proposed, but not previously shown, to be specialized sensors that convert forces into serotonin release, and serotonin released from these cells is important for normal gastrointestinal secretion and motility. The findings in this study show that some enterochromaffin cells are indeed mechanosensitive, and that they use mechanosensitive Piezo2 channels to generate an ionic current that is critical for the intracellular Ca^{2+} increase, serotonin release, and epithelial fluid secretion.

Author contributions: D.R.L., A.B.L., J.H.S., G.F., and A.B. designed research; C.A., K.R.K., A.J.T., G.Y., and P.R.S. performed research; J.H.L. and A.B.L. contributed new reagents/analytic tools; C.A., K.R.K., A.J.T., P.R.S., G.F., and A.B. analyzed data; and C.A., K.R.K., A.J.T., P.R.S., J.H.S., G.F., and A.B. wrote the paper.

The authors declare no conflict of interest.

This article is a PNAS Direct Submission.

[1]To whom correspondence should be addressed. Email: Beyder.Arthur@mayo.edu.

This article contains supporting information online at www.pnas.org/lookup/suppl/doi:10.1073/pnas.1804938115/-/DCSupplemental.

Published online July 23, 2018.

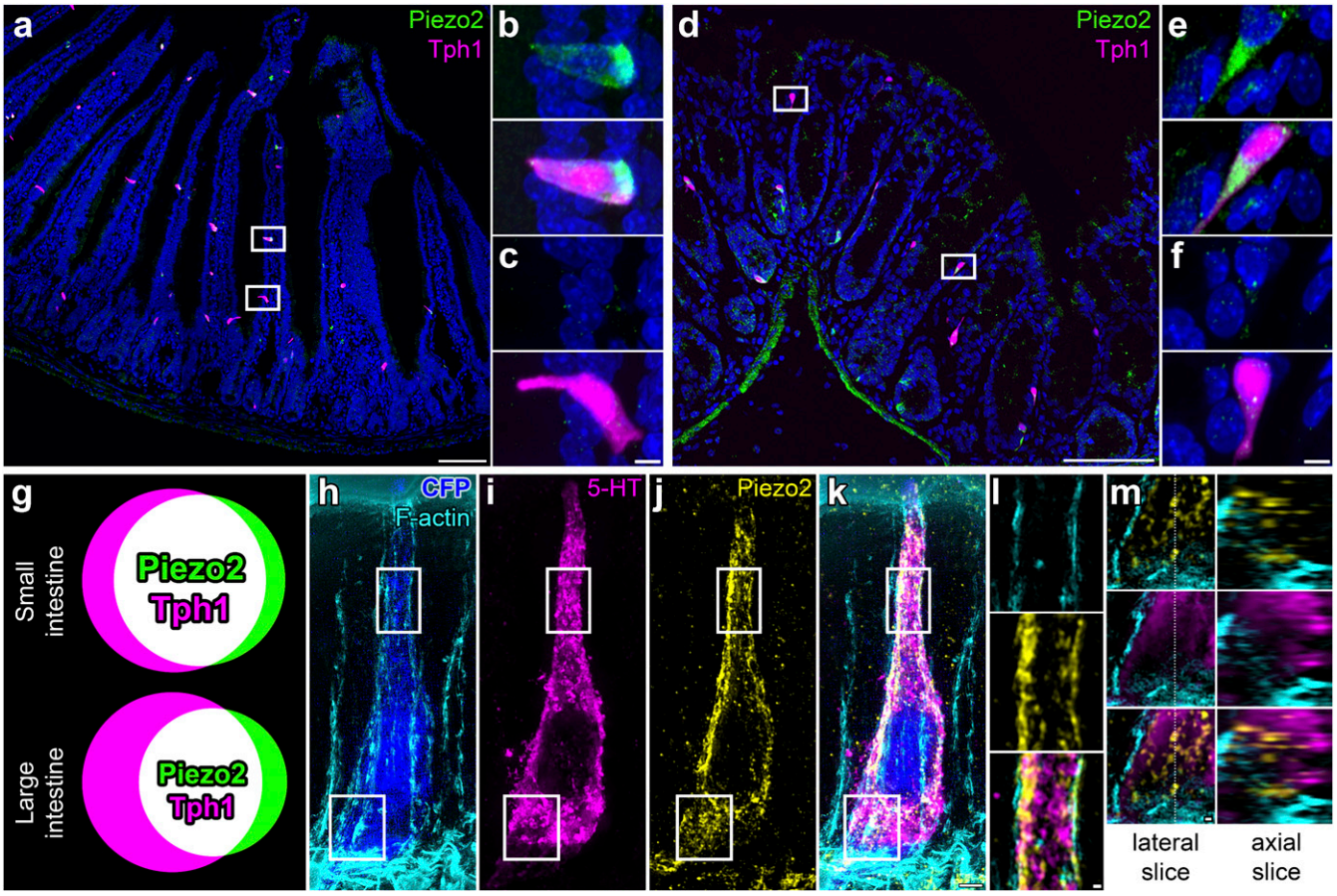

Fig. 1. Piezo2 is a specific marker of an EC cell subset in mouse small and large intestine. (*A–F*) Confocal microscopy of Tph1-CFP mouse small (*A–C*) and large (*D–F*) intestine with CFP labeling Tph1$^+$ EC cells (magenta), Piezo2 immunofluorescence (green), and RedDot2 nuclei (blue). Piezo2 is present in a specific EC cell population in small (*B*) and large (*E*) intestine, and there is a population of EC cells that lack Piezo2 in small (*C*) and large (*F*) intestine. (*G*) Venn diagrams showing the overlap of Piezo2$^+$ (green) and Tph1$^+$ EC (magenta) cells as Piezo2$^+$ Tph1$^+$ EC cells (white) in small and large intestine. (*H–M*) Superresolution SIM of Tph1-CFP mouse jejunum, with (*H*) CFP$^+$ EC cell (blue) and phalloidin-labeling f-actin (cyan), combined with (*I*) immunofluorescence for 5-HT (magenta), (*J*) Piezo2 (yellow), and (*K*) colocalization. (*L*) Membrane-associated Piezo2 localizes near 5-HT vesicles. (*M*) Basal Piezo2 clusters are intracellular and separate form 5-HT vesicles. Images in *A–F* and *H–L* are 2D projections of 3D stacks; in *M* are single imaging planes. [Scale bars: 100 μm (*A* and *D*), 5 μm (*B*, *C*, *E*, and *F*), 2 μm (*H–K*), and 300 nm (*L* and *M*).]

in small and 58 ± 5% in large intestine (n = 203 ± 37 small-intestine cells per mouse, n = 74 ± 33 large-intestine cells per mouse, n = 3) (Fig. 1*G*). Therefore, our data suggest that Piezo2 is specific to a subset of EC cells in both small and large intestine. We used superresolution structured illumination microscopy (SIM) to examine Piezo2 subcellular distribution in EC cells (Fig. 1 *H–M*). We found that Piezo2 was close to cortical f-actin and in close apposition to 5-HT vesicles (Fig. 1*L*), and it was also in discrete intracellular vesicles that were not immunoreactive for 5-HT (Fig. 1*M*).

Lineage-Traced NeuroD1 Cells Are Piezo2$^+$ EE and EC Cells. EC cells constitute the largest population of EE cells (16), but recent studies suggest that the differences between EC and EE cells may be subtler than previously assumed (17, 18). Thus, we utilized *NeuroD1* (19), which is a transcription factor involved in the late stages of EE cell development (18), to create a *NeuroD1-cre;GCaMP5-tdTomato* mouse model in which lineage-traced NeuroD1 cells expressed tdTomato (Fig. 2). We found that 80–83% of EE (CgA$^+$) and 65–79% of EC (5-HT$^+$) cells were NeuroD1$^+$ (tdTomato$^+$) in both small and large intestine, less than 4% of NeuroD1$^+$ cells were CgA$^-$, and we saw no NeuroD1$^+$ cells in the submucosal or myenteric plexus (Fig. 2 *A–C* and *SI Appendix*, Fig. S1). Similar to the Tph1-CFP model (Fig. 1), we found that a subset of NeuroD1$^+$ cells were Piezo2$^+$ (Fig. 2 *D–F*). To examine Piezo2 expression in NeuroD1$^+$ cells, we used a ribosomal trapping approach (20). We created a *NeuroD1-cre; RiboTag* mouse, in which a hemagglutinin (HA) tag was inserted into the coding sequence of ribosomal protein L22 of NeuroD1$^+$ cells (Fig. 2 *G–I*) (20). We examined transcript enrichment in dissociated epithelium (Input) by qRT-PCR of HA affinity-purified or nonspecific mouse IgG control (Ms IgG). We found that HA-purified transcripts were enriched for epithelial (*Vil1*$^+$) EE (*NeuroD1*$^+$, *CgA*$^+$) and EC (*Tph1*$^+$) cell transcripts, as well as Piezo2 (Fig. 2*J*), but not Piezo1 (*SI Appendix*, Fig. S2*A*). These results show that NeuroD1$^+$ cells are EE and EC, and their transcripts are enriched for Piezo2.

NeuroD1$^+$ Cells Have Mechanosensitive Piezo2 Currents. We used the *NeuroD1-cre;GCaMP5-tdTomato* (hereafter, *NeuroD1-GCaMP5*) mouse model to examine whether NeuroD1$^+$ cells are mechanosensitive. We used a method we recently developed to establish mouse primary epithelial cultures (21, 22) and used tdTomato fluorescence to identify NeuroD1$^+$ cells in primary cultures (Fig. 3*A*). We voltage-clamped NeuroD1$^+$ cells and used a piezoelectrically driven glass force probe for mechanical stimulation by membrane displacement (Fig. 3*A*). We found fast mechanosensitive inward currents in 6 of 10 cells (60%) (Fig. 3*B*).

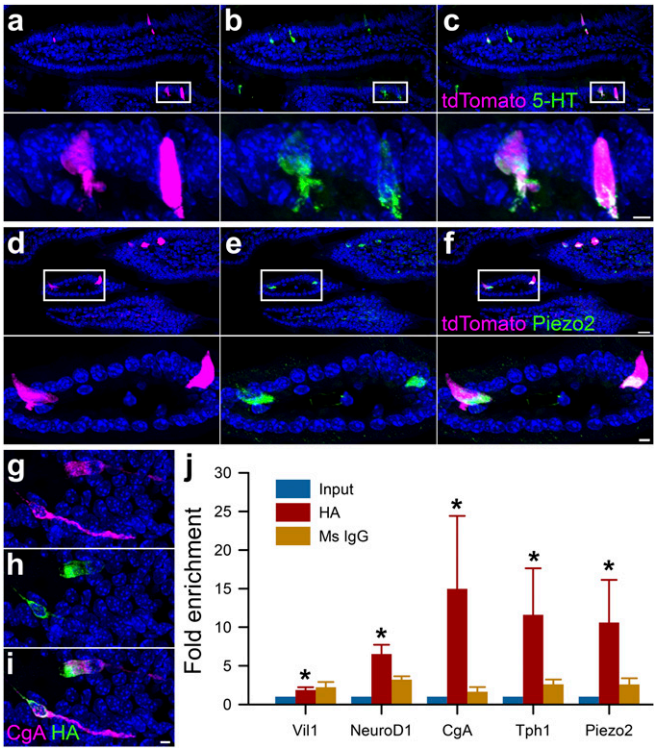

Fig. 2. Lineage-traced NeuroD1 cells are Piezo2$^+$ EE and EC cells. In the *NeuroD1-cre;GCaMP5-tdTomato* mouse the majority of tdTomato$^+$ cells are (*A–C*) 5-HT$^+$ EC cells and (*D* and *E*) Piezo2$^+$. (*A*) tdTomato NeuroD1$^+$ cells (magenta) with (*B*) 5-HT immunofluorescence (green), and (*C*) colocalization. (*D*) tdTomato NeuroD1$^+$ cells (magenta) with (*E*) Piezo2 immunofluorescence (green) and (*F*) colocalization. *Lower* panels are expanded areas from within white rectangles. In *NeuroD1-cre;RiboTag* mouse (*G*) EE cells labeled by chromogranin A (CgA) immunofluorescence (magenta), (*H*) have HA-tagged ribosomes (green), as determined by (*I*) colocalization. [Scale bars: 20 μm (*A–F*) and 5 μm (*A–F*, *Insets* and *G–I*).] (*J*) EE cell mRNA profile from *NeuroD1-cre;RiboTag* mice using qRT-PCR of epithelium (Input, blue), and HA-affinity purification (HA, red) or nontargeted mouse IgG control (Ms IgG, brown). Based on expression, the HA samples are enriched (HA/Input) for epithelial marker *Villin1* (*Vil1*) (HA 2.78-fold over input, $*P < 0.01$), and for EC cell genes *NeuroD1* (HA 6.92-fold $*P < 0.01$), *CgA* (HA 16.14-fold, $*P < 0.01$), *Tph1* (HA 12.12-fold, $*P < 0.01$), and for mechanosensitive ion channel *Piezo2* (HA 12.54-fold, $*P < 0.01$) ($n = 5$ mice).

Nonfluorescent cells in the same preparations did not have such mechanosensitive currents (*SI Appendix*, Fig. S3 *A* and *B*). The NeuroD1$^+$ cell mechanosensitive currents were rapidly activating, reaching peak current in 3.6 ± 0.3 ms and rapidly inactivating with a time constant of inactivation τ_i = 11.4 ± 0.6 ms at peak response ($n = 6$) (Fig. 3*B*), had nonlinear stimulus–response relationships that were fit by a two-state Boltzmann function (Fig. 3*C*), and were nonrectifying, with a linear current–voltage relationship that crossed 0 pA at −4.26 ± 1.34 mV, suggesting a nonselective current (Fig. 3*D*). The NeuroD1$^+$ cell mechanosensitive current biophysical properties were consistent with Piezo2 (13, 23, 24). We attempted to make a NeuroD1$^+$ cell-specific Piezo2 knockout but *NeuroD1-cre;Piezo2$^{f/f}$* mating resulted in a lethal phenotype (*SI Appendix*, Fig. S4). This is likely due to involvement of NeuroD1 in neurogenesis of central nervous system neurons (25) (*SI Appendix*, Fig. S1).

Therefore, we used pharmacological inhibitors and Piezo2 knockdown to test whether the NeuroD1$^+$ cell mechanosensitive currents are Piezo2. In voltage-clamped primary NeuroD1$^+$ cells stimulated by membrane displacement, we found that mechanosensitive currents were inhibited by Gd^{3+}, an established mechanosensitive ion channel blocker (23, 26) and D-GsMTx4, a Piezo1 (27) and Piezo2 (24) blocker (Fig. 3 *E* and *F*). Next we used Piezo2 siRNA to knock down Piezo2 channels. We found that compared with nontargeted (NT) siRNA, Piezo2 siRNA decreased Piezo2 mRNA by 60 ± 10% ($n = 4$, $P < 0.05$), but not Tph1 mRNA ($n = 4$, $P > 0.05$). Piezo2 knockdown by siRNA (11, 23) abolished NeuroD1$^+$ cell mechanosensitive currents unlike NT siRNA (Fig. 3 *E* and *F*), while both retained voltage-dependent currents (21, 28) (*SI Appendix*, Fig. S3*C*). These data show that NeuroD1$^+$ cells have functional Piezo2 mechanosensitive ion channels.

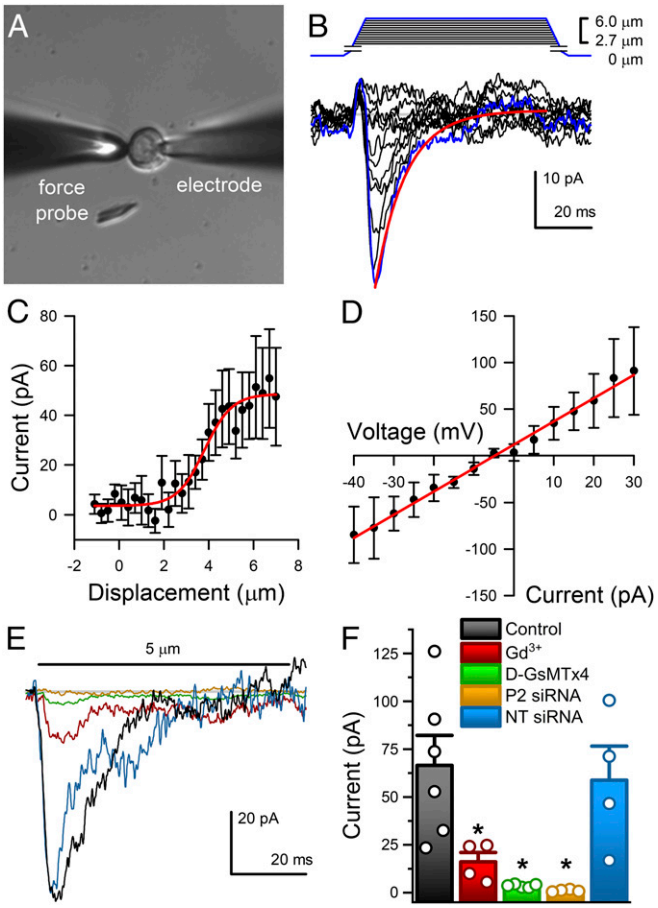

Fig. 3. Piezo2 carries fast mechanosensitive nonrectifying current in NeuroD1$^+$ cells. (*A*) Differential interference contrast (DIC) of a primary EC cell voltage-clamped in whole-cell mode (electrode) and mechanically stimulated by a glass probe (force probe). (Magnification: 40×.) (*B*) Graded increase in cell membrane deformation (0.3 μm per step at −70 mV) results in rapidly activating and inactivating inward currents (peak response, blue trace). (*C*) Peak current (pA) deformation (μm) relationship fit by a two-state Boltzmann function (red) with midpoint (Z_0) 3.46 ± 0.80 μm and slope (dz) 0.79 ± 0.27 ($n = 5$). (*D*) Current–voltage relationship of peak currents in response to 5-μm membrane displacement fit by a linear function (red) with slope (dV) 0.61 ± 0.17 pA/mV and x-intercept (V_0) −4.26 ± 1.34 mV ($n = 5$). (*E*) Typical peak force-induced fast inward currents (black) in EC cells were inhibited by 30 μM Gd^{3+} (red), 10 μM D-GsMTx4 (green), and Piezo2 siRNA (yellow), but not by NT siRNA (blue). (*F*) Individual (circles) and mean ± SEM (bars) peak current (pA) in control EC cells (black, 66.5 ± 15.7 pA, $n = 6$), and significant inhibition of peak current by Gd^{3+} (red, 16.1 ± 4.9 pA, $n = 4$, $*P <$ 0.05, ANOVA with Bonferroni correction), D-GsMTx4 (green, 3.6 ± 0.4 pA, $n = 5$, $*P < 0.05$, ANOVA with Bonferroni correction), and Piezo2 siRNA (yellow, 1.1 ± 0.8 pA, $n = 4$, $*P < 0.05$ compared with NT siRNA, ANOVA), but not NT siRNA (blue, 58.8 ± 17.8 pA, $n = 4$, $P > 0.05$ compared with controls, ANOVA with Bonferroni correction).

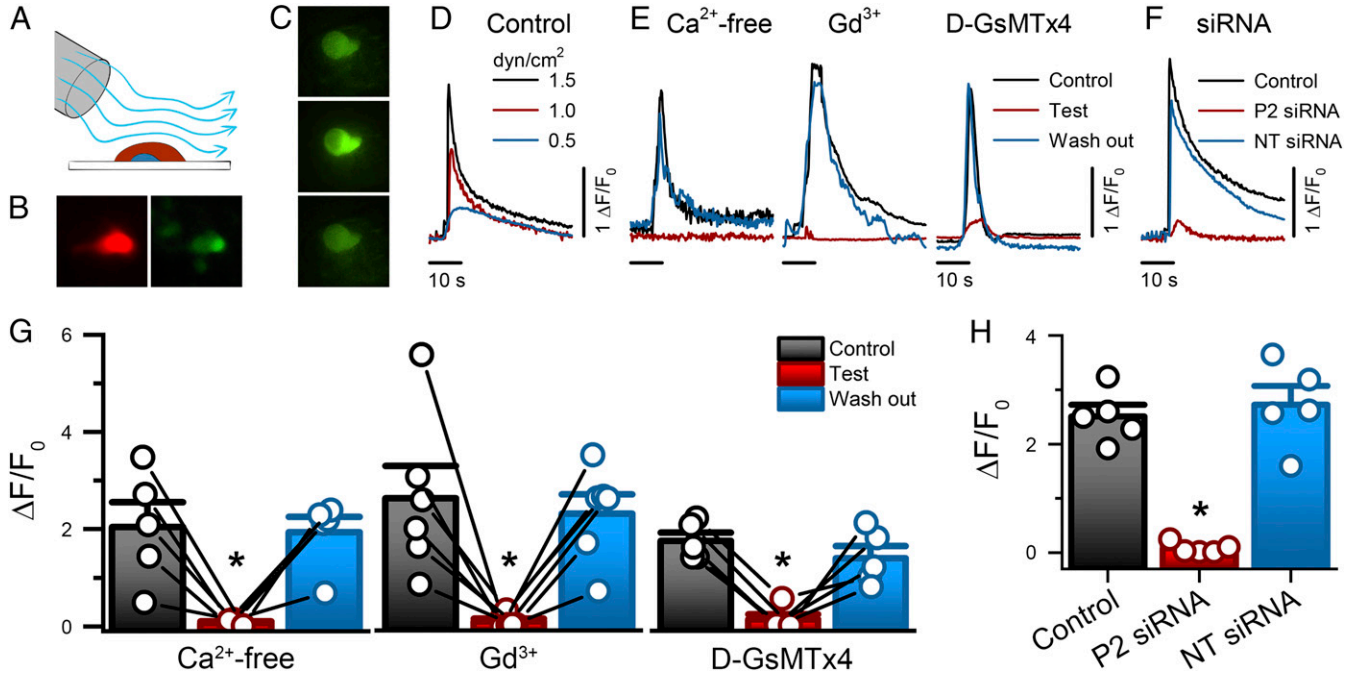

Fig. 4. NeuroD1$^+$ cell stimulation by shear force produces Piezo2-dependent transient intracellular Ca^{2+} increase. (*A*) The experimental set-up used to mechanically stimulate primary EE cells in culture using shear flow by rapid-perfusion system. (*B*) EE cells are identifiable by tdTomato (red) and GCaMP5 (green). (Magnification: 40×.) (*C*) Epifluorescence images of an EE cell GCaMP5 at rest (*Top*), during shear stimulation (*Middle*), and following recovery (*Bottom*). (Magnification: 40×.) (*D*) Representative EE cell GCaMP5 fluorescence fluctuations ($\Delta F/F_0$) elicited by transient shear force (0.5, 1.0, and 1.5 dyn/cm^2). (*E*) Representative traces of GCaMP5 fluorescence in response to shear force (1.5 dyn/cm^2) in the absence (Control, black), presence (Test, red), and following recovery (wash-out, blue) of Ca^{2+}-free extracellular solution, 30 μM Gd^{3+}, and 10 μM D-GsMTx4. (*F*) Representative traces of GCaMP5 fluorescence elicited by shear force in Piezo2 siRNA (P2 siRNA), NT siRNA, and Control cells. (*G*) Individual (circles) and mean ± SEM (bars) NeuroD1$^+$ cell GCaMP5 responses ($\Delta F/F_0$) for Ca^{2+} free extracellular solution (control 2.0 ± 0.5, Ca^{2+}-free 0.1 ± 0.02, wash-out 1.9 ± 0.3, $n = 5$), 30 μM Gd^{3+} (control 2.6 ± 0.7, Gd^{3+} 0.09 ± 0.05, wash-out 2.3 ± 0.4, $n = 6$) and 10 μM D-GsMTx4 (control 1.7 ± 0.2, D-GsMTx4 0.1 ± 0.1, wash-out 1.4 ± 0.2, $n = 5$). *$P < 0.05$, Tukey test with multiple comparisons. (*H*) Individual (circles) and mean ± SEM (bars) NeuroD1$^+$ cell GCaMP5 responses ($\Delta F/F_0$) for nontransfected Control (2.5 ± 0.2, $n = 5$), Piezo2 siRNA-transfected (P2 siRNA, 0.08 ± 0.05, $n = 5$) and NT siRNA-transfected (2.7 ± 0.3, $n = 5$). *$P < 0.05$ for Piezo2 siRNA compared with control and NT siRNA, ANOVA with Bonferroni correction.

Piezo2 Is Necessary for Mechanosensitive Intracellular Ca^{2+} Increase in NeuroD1$^+$ Cells. We wondered whether Ca^{2+} signaling was downstream of Piezo2 activation by physiologically relevant stimuli in mechanosensitive NeuroD1$^+$ cells. We used a rapid perfusion system to apply shear force, a highly relevant stimulus for GI epithelium, on primary cultured NeuroD1$^+$ cells from *NeuroD1-GCaMP5* mouse (Fig. 4*A*), which are tdTomato$^+$ (Fig. 4*B*) and GCaMP5$^+$ (Fig. 4*C*). Of the stimulated NeuroD1$^+$ cells, 58% (34 of 59) responded to 20-s shear force with a prolonged stimulus-dependent increase in intracellular Ca^{2+} of more than 200% ($\Delta F/F_0$ 2.15 ± 0.5, time to peak 8.8 ± 1.2 s, $n = 8$, return to baseline ~60 s, $n = 12$) (Fig. 4 *C* and *D* and Movie S1), which was comparable to chemical stimulation by KCl (*SI Appendix*, Fig. S5 *A–C*). Shear-induced Ca^{2+} increases were reversibly inhibited by Ca^{2+}-free media, mechanosensitive channel blocker Gd^{3+}, and Piezo channel inhibitor D-GsMTx4 (Fig. 4 *E* and *G* and *SI Appendix*, Fig. S5*A*), but Piezo1 chemical stimulator Yoda1 did not influence NeuroD1$^+$ cell Ca^{2+} (*SI Appendix*, Fig. S2 *B* and *C*). Piezo2 knockdown by Piezo2 siRNA, but not NT siRNA, diminished shear-induced Ca^{2+} increase (Fig. 4 *F* and *H*). In addition to KCl responsiveness, Piezo2 siRNA- and NT siRNA-treated cells retained responses to allyl isothianate (AITC), which activates TRPA1 channels that are specific to EC cells (28, 29) (*SI Appendix*, Fig. S5 *D* and *E*). These data show that mechanical stimulation of primary NeuroD1$^+$ leads to Piezo2-dependent intracellular Ca^{2+} increase.

NeuroD1$^+$ Cells' Mechanosensitivity in the Epithelium Is Piezo2-Dependent. We next asked whether NeuroD1$^+$ cells were mechanosensitive within the epithelium. Using *NeuroD1-GCaMP5* mice, we established intestinal organoids, which are self-organizing 3D in vitro GI epithelial models that contain all known epithelial cell types (*SI Appendix*, Fig. S6 *A–C*) (30). However, the 3D structure prevents well-defined mechanical stimulation. We developed a protocol, similar to others (31), to "planarize" the organoids into monolayers (Fig. 5 *A–C* and *SI Appendix*, Fig. S6 *D–G*). Planarized organoids maintained Piezo2-expressing tdTomato$^+$ EC cells (Fig. 5 *A–C* and *SI Appendix*, Fig. S6). We stimulated the planarized organoids with shear force (Fig. 5*D*) and found that as in isolated NeuroD1$^+$ cells, shear force evoked an increase in intracellular Ca^{2+} (Fig. 5*D* and Movie S2). To test if Piezo2 channels were involved, we blocked them with D-GsMTx4 or knocked them down with Piezo2 siRNA and found a decrease of shear-force responses compared with controls and NT siRNA, respectively (Fig. 5 *E* and *F*). These data suggest that NeuroD1$^+$ cells are mechanosensitive within intact GI epithelium.

Mechanically Induced EC Cell 5-HT Release Depends on Piezo2. Having established that EE cells are mechanosensitive, we wanted to know whether the 5-HT–releasing EE cells—the EC cells—are mechanosensitive, if EC cell mechanical stimulation resulted in 5-HT release, and if Piezo2 was involved. We used primary *NeuroD1-GCaMP5* cultures to assay EC cell 5-HT release from NeuroD1$^+$ cells in response to membrane displacement using a "5-HT biosensor," an engineered HEK-293 cell with genetically modified 5-HT–gated ion channel (5-HT_3R) and GCaMP5G (Fig. 6 *A* and *B*). Because 5-HT_3R desensitize within milliseconds, we used a genetically engineered 5-HT_3R with large single-channel

PHYSIOLOGY

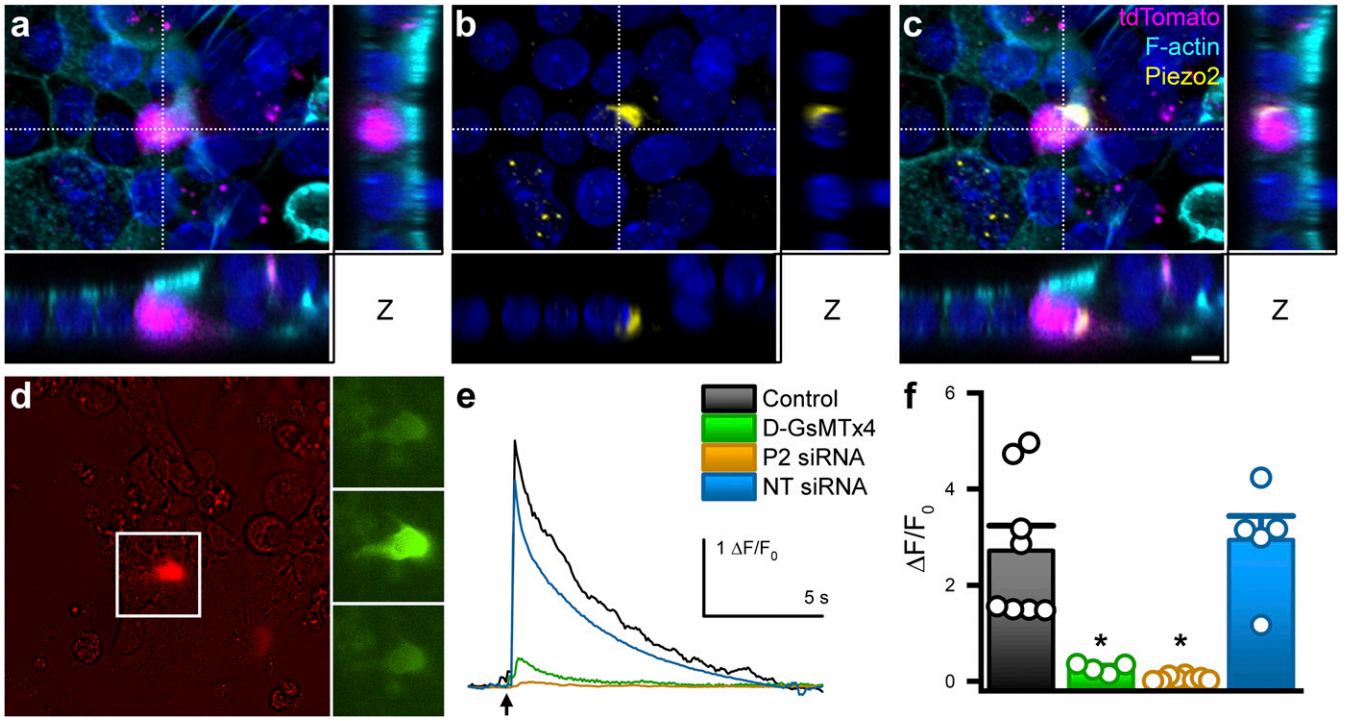

Fig. 5. NeuroD1$^+$ cells within intact epithelium depend on Piezo2 for mechanosensitivity. (*A*) Confocal imaging of a typical planar organoid generated from *NeuroD1-cre;GCaMP5-tdTomato* mouse small intestine with an EC cell (magenta), phalloidin (cyan), and DAPI (blue) labeling. Monolayer organization is demonstrated by orthogonal views derived from the areas highlighted by the dashed cross-hairs to the right (vertical line) and below (horizontal line). (*B*) Piezo2 immunofluorescence (yellow), with *C*, colocalization of Piezo2 and tdTomato labeling. Voxel size $x,y = 265$ nm; $z = 350$ nm. [Scale bar (applies to *A–C*), 5 μm.] (*D*) Overlaid DIC/epifluorescence image of planar epithelial organoids showing EC cells (tdTomato, *Right*) and GCaMP5 at rest (*Top*), during shear force stimulation (*Middle*), and after recovery (*Bottom*). (*E*) Representative Ca^{2+} (GCaMP5) responses ($\Delta F/F_0$) to shear-force stimulation of NeuroD1$^+$ cells within planar organoids with Control solution (black), in the presence of 10 μM D-GsMTx4 (green) and transfected with Piezo2 siRNA (brown) and NT siRNA (blue). (*F*) Individual (circles) and mean ± SEM (bars) peak Ca^{2+} ($\Delta F/F_0$) responses for Control shear (2.7 ± 0.5, $n = 8$, black), 10 μM D-GsMTx4 (0.3 ± 0.05, $n = 4$, green), Piezo2 siRNA (P2 siRNA, 0.06 ± 0.02, $n = 8$, brown), and NT siRNA (2.9 ± 0.5, $n = 5$, blue) in planar organoids (*$P < 0.05$ paired *t* test for Gd^{3+} and D-GsMTx4 vs. Control, and unpaired *t* test for Piezo2 siRNA vs. NT siRNA).

current and no desensitization (*SI Appendix*, Fig. S7 *A–C*) (32). We found that in 77% (17 of 22) of mechanosensitive NeuroD1$^+$ cells from *NeuroD1-GCaMP5* cultures mechanical stimulation evoked an intracellular Ca^{2+} increase (time to peak 2.4 ± 0.4 s, $n = 5$) (Fig. 6 *C*, *E*, and *G*, black) and 5-HT release detected by 5-HT biosensors after a diffusion-limited delay (Fig. 6 *D*, *F*, and *H*, black, and Movie S3). Therefore, these NeuroD1$^+$ cells are mechanosensitive EC cells. To determine the specificity of the 5-HT biosensor responses, we used the 5-HT_3R antagonist ondansetron and found that, whereas the EC cells continued to respond to mechanical stimulus (Fig. 6 *E* and *G*, red), 5-HT biosensors did not (Fig. 6 *F* and *H*, red, and *SI Appendix*, Fig. S7 *B* and *C*). To test whether Piezo2 channels were responsible for mechanosensitive 5-HT release from EC cells, we used the Piezo channel blocker D-GsMTx4, Piezo2 siRNA, and NT siRNA, and found that D-GsMTx4 (green in Fig. 6) and Piezo2 siRNA (brown in Fig. 6) decreased both EC cell responses to force (Fig. 6 *E* and *G*) and the 5-HT biosensor responses (Fig. 6 *F* and *H* and *SI Appendix*, Fig. S7 *B* and *C*), while NT siRNA (blue in Fig. 6 *E–H*) did not. Piezo2 siRNA-treated EC cells retained their chemosensitive responses to TRPA1 agonist AITC (*SI Appendix*, Fig. S7 *D* and *E*). These results suggest that in mechanosensitive EC cells, force-induced Piezo2-dependent intracellular Ca^{2+} increase leads to 5-HT release.

Epithelial Piezo2 Knockout Decreases Mechanosensitive Epithelial Secretion. To test the EC cell Piezo2 role in GI physiology, we used the GI epithelial driver *Vil-cre* (*SI Appendix*, Fig. S8) to create conditional GI epithelium-specific Piezo2 knockout $Piezo2^{CKO}$ (*Vil-cre;*$Piezo2^{f/f}$) (*SI Appendix*, Fig. S9) and compared it to littermate control $Piezo2^{WT}$ ($Piezo2^{f/f}$).

To determine whether epithelial Piezo2 contributes to pressure-induced secretion, we used a custom Üssing chamber, in which we are able to apply simultaneous pressure- and voltage-clamps (11) and measure pressure-induced epithelial short-circuit currents (I_{sc}), which is a surrogate for epithelial secretion (Fig. 7*A*) (33). We tested the hypothesis that luminal mechanical stimulation leads to EC cell Piezo2-dependent epithelial fluid secretion by a previously established secretion circuit that relies on epithelial 5-HT (Fig. 7*B*) (3, 4, 11). When we pressurized the epithelial side in steps of increasing amplitude in $Piezo2^{WT}$, we found that increasing pressure resulted in a stimulus-dependent I_{sc} increase (black traces in Fig. 7 *C* and *D*). Compared with $Piezo2^{WT}$, the $Piezo2^{CKO}$ mice had a significantly decreased pressure-induced I_{sc} (red traces in Fig. 7 *C* and *D*). Secretion response to acetylcholine was not different between $Piezo2^{WT}$ and $Piezo2^{CKO}$ ($n = 15$, $P > 0.05$) (Fig. 7*C*). Inhibition of pressure-induced secretion was not complete in $Piezo2^{CKO}$ compared with $Piezo2^{WT}$. Thus, we compared the pressure-induced secretion responses to inhibitor D-GsMTx4 in both models. We found that D-GsMTx4 inhibited pressure-induced secretion response in $Piezo2^{WT}$ ($P2^{WT}$) but not in $Piezo2^{CKO}$ ($P2^{CKO}$) (Fig. 7 *E* and *F*). These results suggest that EC cell Piezo2 is important for mechanically induced epithelium secretion.

Discussion

Orchestrated GI secretion and motility are critical for normal digestion. These GI functions are regulated by the coordinated responses to intraluminal nutrients and mechanical forces. Epithelial EE and EC cells sense nutrients and metabolites, and coordinate physiologic responses (28, 34). EC cells, the most common type of EE cells (16), were proposed to be specialized mechanosensors that in response to force release 5-HT (1, 2), which stimulates secretory reflexes (3, 4). However, EC cell mechanosensitivity was inferred from studies on intact tissues (2, 35) and cell models (9–11, 24). In this study we addressed critical knowledge gaps: whether EE and EC cells are mechanosensitive and, if so, what is the mechanism of their mechanosensitivity?

We found that mechanosensitive ion channel Piezo2 was specific (~80%) for EC cells in both small and large intestine of a *Tph1-CFP* mouse model (15), which is similar to Piezo2 specificity for human small-intestine EC cells (11). Interestingly, Piezo2 was not present in all EC cells: Piezo2$^+$ EC cells constituted a subset of ~60–70% of EC cells. Recent studies show that the differences between EC and EE cells may be subtler than previously assumed (18, 36). EC cells express enzymes required to produce signaling molecules other than 5-HT, such as secretin and substance P (18, 36), and even contain endocrine hormones, such as CCK, GLP-1, and somatostatin, that were previously ascribed to other EE cells (37). Thus, we lineage-traced all EE cells using *NeuroD1-cre*, because *NeuroD1* is a transcription factor that is a "late" determinant for EE cell differentiation (18, 38). We found that NeuroD1$^+$ cells were EE and EC cells and, importantly, they did not include non-EE secretory cells, such as goblet and Paneth cells. Like in the *Tph1-CFP* mouse, we found that a subset of NeuroD1$^+$ EC cells was Piezo2$^+$, and that Piezo2 mRNA, as well as EE and EC cell-specific mRNAs, were enriched within NeuroD1$^+$ cell transcripts. These results suggested that a well-defined subset of Piezo2$^+$ EE and EC cells may be mechanosensitive. Consistent with the immunofluorescence, lineage tracing, and expression results, functional experiments showed that ~60% of primary EE cells had Piezo2-dependent mechanosensitivity when examined by electrophysiology and Ca^{2+} imaging. Furthermore, using 5-HT biosensors and the EC cell-specific TRPA1 chemical activator (28, 29), we found that mechanosensitive Piezo2$^+$ 5-HT–releasing EC cells made up the largest subset (~80%) of mechanosensitive EE cells.

EC cell 5-HT has neuroepithelial (28) and endocrine (7, 39) roles. Mechanosensitive 5-HT release from intestinal mucosa has a rapid-rise phase measured in milliseconds (2, 40), presumably for neuroepithelial communication (28). This speed is consistent with the fast Piezo2 kinetics (23, 41). We found that EC cell Piezo2 was distributed at high densities near cortical f-actin, suggesting membrane localization, and close to 5-HT vesicles, which suggested functional coupling. Mechanosensitive EE cells had nonrectifying mechanosensitive currents that activated and inactivated within tens of milliseconds. These mechanosensitive currents resembled heterologously expressed Piezo2 currents (23), and Piezo2 currents in Merkel cells (13, 42) and neurons (43, 44). They were inhibited by Piezo pharmacological blockers and Piezo2 knockdown by siRNA. Furthermore, Piezo2-dependent mechanosensitive 5-HT release by EC cells was also fast, limited only by diffusion.

In addition to the rapid onset, EC cell 5-HT release also has a prolonged phase lasting many seconds (2, 40), which likely contributes to EC cell endocrine function (7, 39). The lengthy 5-HT release in response to force was surprising given rapid inactivation of Piezo2 (23, 41). Because the previous studies were done in intact tissues, it was possible that the prolonged responses to force depended on the enteric nervous system (ENS) (40, 45). However, we found that mechanical stimulation by rapid membrane displacement (50 ms) or longer-lasting shear stress (20 s) of isolated EE cells in intact intestinal organoids that lack ENS, resulted in intracellular Ca^{2+} increases that lasted many seconds and depended on Piezo2 and extracellular Ca^{2+}. When we focused on EC cells using biosensors to detect single-cell 5-HT release (46), we again found that brief EC cell mechanical stimulation led to Piezo2-dependent intracellular Ca^{2+} increase and was followed by 5-HT release that was rapid in onset and lasted several seconds. These findings suggest that mechanosensitive EC cells amplify Piezo2 responses to force into temporally controlled 5-HT release.

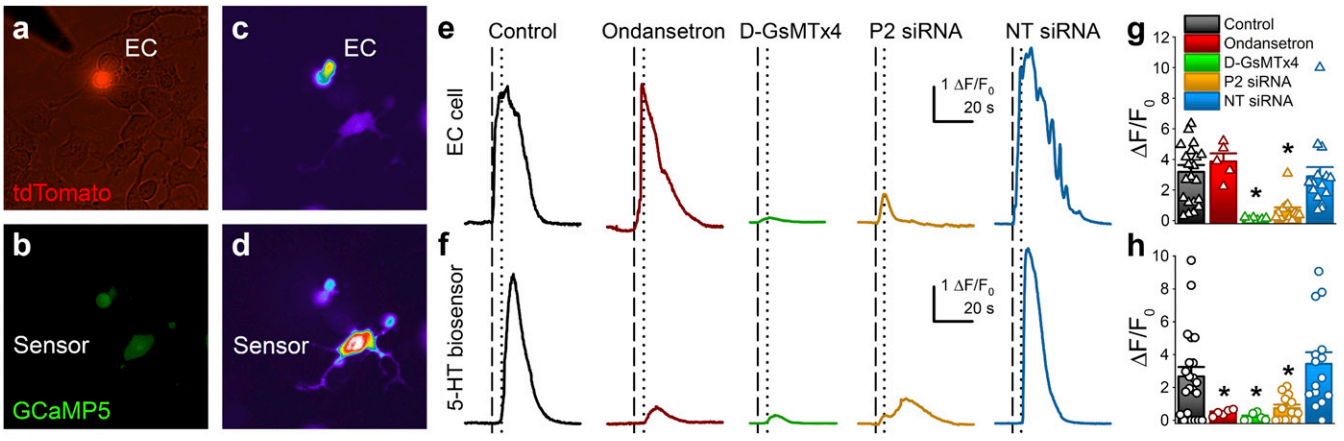

Fig. 6. Mechanosensitive EC cell 5-HT release depends on Piezo2. (*A*) 5-HT biosensor experiment showing overlaid DIC/tdTomato images with an EC cell, and (*B*) GCaMP5 in both the EC and 5-HT biosensor cell (lower part of image). EC cell mechanical stimulation by force probe results in (*C*) Ca^{2+} increase in EC cell, and (*D*) later in 5-HT biosensor. (*E*) Representative traces of Ca^{2+} responses ($\Delta F/F_0$) during EC cell mechanical stimulation, and *F*, resulting 5-HT biosensor activity in a control experiment (black), with 0.1 μM ondansetron (red), 10 μM D-GsMTx4 (green), Piezo2 siRNA (brown), and NT siRNA (blue). Vertical lines represent stimulation of EC cell (dashed) and initiation of 5-HT biosensor cell response (dotted). (*G*) Individual (NeuroD1$^+$ cells triangles, 5-HT biosensors circles) and mean ± SEM (bars) Ca^{2+} responses ($\Delta F/F_0$) of EC cell mechanical stimulation and (*H*) resulting 5-HT biosensor cell activity in controls (EC cell: 3.2 ± 0.5, $n = 22$ and 5-HT biosensor: 2.7 ± 0.6, $n = 22$), with ondansetron (EC cell: 3.9 ± 0.5, $n = 5$ and 5-HT biosensor: 0.5 ± 0.1, $n = 5$), with D-GsMTx4 (EC cell: 0.1 ± 0.03, $n = 6$, and 5-HT biosensor: 0.19 ± 0.09, $n = 6$), with Piezo2 siRNA (EC cell: 0.6 ± 0.2, $n = 13$, and 5-HT biosensor: 0.7 ± 0.2, $n = 13$), and with NT siRNA (EC cell: 2.9 ± 0.4, $n = 15$, and 5-HT biosensor: 3.3 ± 0.7, $n = 15$) (*$P < 0.05$ when comparing D-GsMTx4 to control, and Piezo2 siRNA to NT siRNA for EC cell and biosensor cell, and when comparing ondansetron and D-GsMTx4 to control for biosensor cell only, by unpaired *t* test).

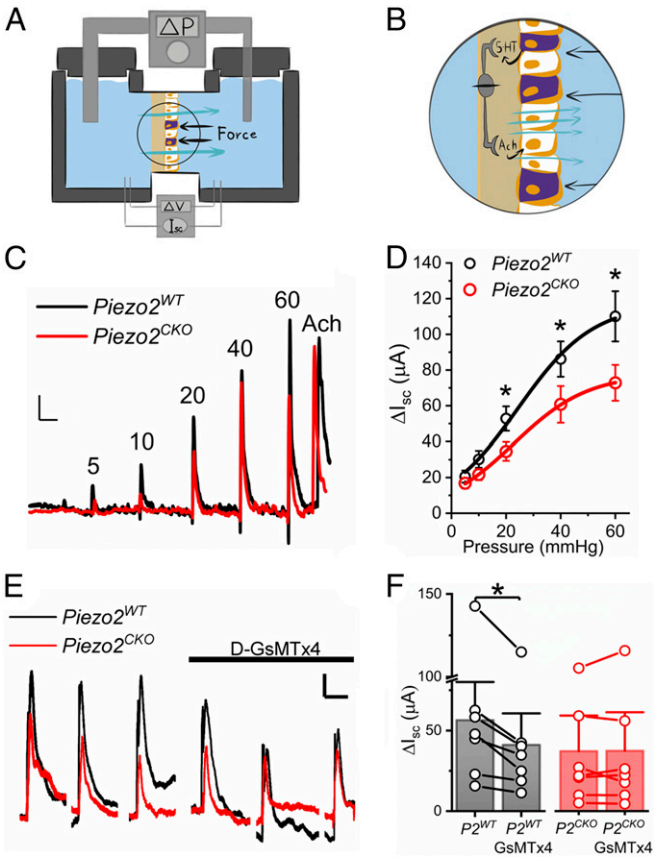

Fig. 7. Pressure-induced mucosal secretion depends on epithelial Piezo2. (*A*) Cartoon of the experimental Üssing chamber set-up for epithelial pressure-clamp (ΔP) and voltage-clamp (ΔV) to measure pressure-induced epithelial secretion via short-circuit current (I_{sc}). Black arrows represent pressure; cyan arrows represent secretion. (*B*) Circled area in *A* enlarged to show full-thickness gut segment mounted in Üssing chamber with hydrostatic pressure (black arrows) stimulation that leads to pressure-induced 5-HT release and activation of IPANs that stimulate secretomotor neurons to produce ACh-induced activation of epithelial secretion (cyan arrows). (*C*) Representative short-circuit current (I_{sc}) traces showing increases in control (*Piezo2*^{WT}, black) and *Piezo2*^{CKO} (red) jejunum at incremental pressure steps (ΔP, 10 s) of 5, 10, 20, 40, and 60 mmHg, followed by ACh as a positive control to test tissue viability. (Scale bars: 20 μA and 120 s.) (*D*) Mean ± SEM short-circuit current (I_{sc}) in response to pressure (ΔP) in control (*Piezo2*^{WT}, black) and epithelial *Piezo2*^{CKO} (red) for 5 mmHg (20.56 ± 3.37 μA vs. 16.83 ± 2.97 μA), 10 mmHg (30.18 ± 4.74 μA vs. 21.69 ± 3.20 μA), 20 mmHg (52.84 ± 6.81 μA vs. 34.55 ± 5.21 μA), 40 mmHg (86.16 ± 9.92 μA vs. 60.77 ± 10.26 μA), and 60 mmHg (110.09 ± 14.06 μA vs. 72.83 ± 10.04 μA) (n = 15 each, $^*P < 0.05$, paired t test). (*E*) Representative traces showing I_{sc} of control (*Piezo2*^{WT}, black) and *Piezo2*^{CKO} (red) jejunum responses to three 10-s 20-mmHg pressure steps (ΔP) with and without D-GsMTx4. (Scale bars: 5 μA and 60 s.) (*F*) Individual points (circles) and mean ± SEM (bars). I_{sc} in *Piezo2*^{WT} jejunum in the absence (*P2*^{WT}, 56.4 ± 15.8 μA) and presence of D-GsMTx4 (*P2*^{WT}*+GsMTx4*, 41.1 ± 13.0 μA) (n = 7, $^*P < 0.05$, paired t test) and *Piezo2*^{CKO} jejunum in the absence (*P2*^{CKO}, 36.3 ± 14.4 μA) and presence of D-GsMTx4 (*P2*^{CKO}*+GsMTx4*, 36.5 ± 15.5 μA) (n = 7, $P > 0.05$, paired t test).

The mechanotransduction mechanism linking Piezo2 with intracellular Ca^{2+} increase and 5-HT release requires further clarification. Because EE and EC cells are electrically excitable (21, 28, 47), it is possible that Piezo2 generates a receptor potential that activates voltage-gated sodium channels, which mediate seconds-long EC cell-bursting activity (21, 28), and activate voltage-gated calcium channels, which have been implicated in EC cell chemosensitivity (28, 48, 49). Another possibility is that Ca^{2+} flux through Piezo2 directly activates EC cell Ca^{2+}-induced Ca^{2+} release (50) or ATP release and subsequent autocrine P2X activation (51). These possibilities are not mutually exclusive, and clarifying the involvement of these mechanisms in EC mechanotransduction may help delineate EC cell roles within the neuroepithelial (28, 52) and endocrine (7, 39) systems.

To examine the physiological role of Piezo2 in EC cell mechanosensitivity, we made a conditional GI epithelium Piezo2 knockout (*Piezo2*^{CKO}). EC cell 5-HT is important in pressure-induced secretion responses (3, 4), and mucosal pressure increases both 5-HT release and short-circuit current (I_{sc}), a surrogate for epithelial secretion (11). Thus, we compared with *Piezo2*^{WT}, the *Piezo2*^{CKO} pressure- and voltage-clamped small intestine, and found that *Piezo2*^{CKO} had a diminished pressure-induced short-circuit current at multiple pressures. Pressure sensitivity was not further decreased by Piezo blocker D-GsMTx4 in *Piezo2*^{CKO} compared to *Piezo2*^{WT}. Our results suggest that EC cell Piezo2 is responsible for a portion, but not all, pressure-induced secretion response. This is intriguingly akin to the results found in somatosensory light touch, where Piezo2 deletion in both Merkel cells and afferent neurons is required for complete sensory loss (43). In the GI system, EC cells communicate with intrinsic primary afferent sensory neurons (IPANs), which were previously described to be mechanosensitive (53). Further work is required to determine the identity of the IPAN mechanotransducer, and whether inhibition of IPAN and EC cell mechanosensitivity leads to a more complete mechanosensory loss.

In summary, we show here that subsets of primary EE and EC cells are mechanosensitive, that their mechanosensation requires Piezo2 channels, the activation of which by force leads to a rapid ionic current, mechanosensitive intracellular Ca^{2+} increase, mechanosensitive 5-HT release from EC cells, and pressure-induced epithelial fluid secretion.

Methods

All experimental procedures were approved by the Institutional Animal Care and Use Committee of the Mayo Clinic.

Drugs. Gadolinium (Gd^{3+}), 5-HT, AITC, and ondansetron (Sigma-Aldrich), Yoda1 (21904; Cayman Chemical) were all made as stock solutions (1 mM) in water. Working solutions were prepared from stock on the day of the experiments, and D-GsMTx4 (provided by Philip Gottlieb, State University of New York, Buffalo, NY) was made as a working solution on the day of the experiments.

Animals. *Piezo2*$^{f/f}$ mice were provided by Ardem Patapoutian, The Scripps Research Institute, San Diego, CA. *NeuroD1-cre* and *Tph1-CFP* mice were provided by Andrew Leiter, University of Massachusetts, Worcester, MA. Mouse lines obtained from The Jackson Laboratories were: *Vil-cre* (Jax 021504), *Ai9* (Jax 007909), *RiboTag* (Jax 011029), and *tdTomato-GCaMP5* (Jax 024477).

Cultures.

Primary murine colon dissociation. Primary murine colon dissociation was similar to recently described work (21, 22); *NeuroD1-GCaMP5* mice were killed at 5–7 wk and a 10-cm length of colon was removed. Full-thickness tissue was inverted, chopped, and washed three times in ice-cold PBS. The tissue was digested under agitation at 37 °C in DMEM (Sigma), 0.1% BSA (Sigma), and 0.6 mg/mL Collagenase type XI (C9407; Sigma) in four separate digestions, for a total of 40 min. Supernatants were collected from the last two digestions, spun twice at 100 × *g* for 5 min, and suspended at 1,000,000 cells per milliliter in DMEM, 5% heat-inactivated FBS (F4135; Sigma), 1% Pen-step (Invitrogen), 1% L-Glutamine (Invitrogen) in dishes (MatTek Corporation) coated with 5% (wt/vol) Matrigel (Corning). Cells were maintained in standard culture conditions for 24–48 h.

siRNA. siRNA transfection efficiency was optimized using siGLO Green Transfection Indicator (D-001630-01-05; Dharmacon) transfected using Lipofectamine 2000 (Invitrogen). For primary cell culture siRNA experiments, FBS and Matrigel concentrations were dropped to 2.5%. When noted, 20 nM siRNA Accell Mouse Piezo2 siRNA–SMARTpool (E-163012-00-0005; Dharmacon) or 20 nM Accell Nontargeting Control siRNA (D-001910-10-05; Dharmacon) were transfected for 48–72 h.

Murine jejunum organoids. Organoids were cultured and maintained according to Intesticult Organoid Growth Medium (StemCell) instructions. *NeuroD1-GCaMP5*

mice were killed at 8–10 wk, and a 20-cm length of small intestine was removed. The segment was cut open lengthwise, flushed with PBS, and then cut into 2-cm pieces. The tissue pieces were resuspended in PBS and pipetted with fresh buffer until the supernatant was clear. Tissue pieces were resuspended in Gentle Cell Dissociation Reagent (StemCell) and incubated on a rocking shaker at room temperature for 15 min. Dissociation reagent was removed and PBS containing 0.1% BSA was added to the tissue. Tissue pieces were then pipetted up and down three times in the buffer and this was repeated four times to generate different four fractions. The first two fractions were discarded and the last two were collected, filtered, and spun at 300 × *g*. Both fractions were combined in DMEM/F12 (Sigma), counted, spun again, and resuspended in equal parts of room temperature Intesticult Organoid Growth Medium and Matrigel Growth Factor Reduced Basement Membrane Matrix (Corning) at a density of 5,000 crypts per six wells in prewarmed 24-well dishes (Corning).

Organoids were grown under standard cell culture conditions and Intesticult Organoid Growth Medium was replaced every 3 d. After 7 d in culture, the organoids were passaged. Gentle Cell Dissociation Reagent was used to break up the organoid domes and then incubated on a rocking shaker at room temperature for 10 min. The organoid fragments were spun at 300 × *g*, resuspended in DMEM/F12, counted, spun again, and resuspended in equal parts of room temperature Intesticult Organoid Growth Medium and Matrigel Growth Factor Reduced Basement Membrane Matrix at a density of 5000 crypts per six wells in prewarmed 24-well dishes. Planar organoids were plated in Intesticult Organoid Growth Medium at a density of 1,000 organoid fragments per dish in Mattek dishes precoated with 5% (wt/vol) Matrigel Growth Factor Reduced Basement Membrane Matrix. When noted, 20 nM siRNA Accell Mouse Piezo2 siRNA–SMARTpool (E-163012–00-0005; Dharmacon) or 20 nM Accell Nontargeting Control siRNA (D-001910-10-05; Dharmacon) were transfected for 24–72 h (Invitrogen). For planar organoid siRNA experiments, Matrigel concentration was dropped to 2.5%.

Gene Expression.

RNA isolation. Ribotag protocols were modified from previous studies (20). Colon tissue was harvested from 6- to 10-wk-old NeuroD1-RiboTag mice. Epithelial tissue was isolated by placing full-thickness tissue in Dulbecco's PBS supplemented with EDTA (2 mM) and DTT (1 mM) and incubated at 37 °C for 20 min. Tissue was shaken vigorously, spun at 1,000 × *g*, and the pellet was collected. Samples were prepared by homogenizing the epithelial tissue pellet with homogenization buffer (50 mM Tris, pH 7.5, 100 mM KCl, 12 mM Mg Cl_2, 1% Nonidet P-40, 1 mM DTT, 200 U/mL Promega RNasin, 1 mg/mL heparin, 100 μg/mL cycloheximide, Sigma protease inhibitor mixture). Samples were centrifuged for 10,000 × *g* for 10 min to create a postmitochondrial supernatant. Next, 100 μL of the supernatant was frozen and stored at −80 °C until further RNA processing. The remaining supernatant was divided and incubated overnight with either a mouse monoclonal anti-HA antibody (901513; Biolegend) or Mouse IgG (MABF1081Z; Millipore) coupled to Protein G magnetic beads (Dynabeads; Invitrogen). After overnight incubation, the beads were washed three times for a total of 30 min in a high-salt buffer (50 mM Tris, pH 7.5, 300 mM KCl, 12 mM MgCl2, 1% Nonidet P-40, 1 mM DTT, 100 μg/mL cycloheximide). RLT buffer (RNeasy Plus Mini Kit; Qiagen) supplemented with β-mercaptoethanol was added to each sample and then vortexed for 30-s RNA isolation was then performed on all samples using the RNeasy Plus Mini Kit (Qiagen).

qRT-PCR. RNA was collected from either RiboTag experiments or siRNA treated primary cell cultures. Reverse transcription of the RNA was completed by using SuperScript VILO cDNA Synthesis Kit (Invitrogen) and a PCR of 10 min at 25 °C, a 60 min cycle at 42 °C, and 5 min at 85 °C. For Piezo2 siRNA knockdown analysis, cDNA was diluted and analyzed for GAPDH, HPRT, and Piezo2$^{\#}$ (*SI Appendix*, Table S1). For RiboTag, cDNA was diluted and analyzed for GAPDH, HPRT, Piezo2, Vil1, Tph1, CgA, and NeuroD1 (*SI Appendix*, Table S1). Both experiments were done by qRT-PCR according to LightCycler 480 SYBR Green I Master (Roche) instructions.

Immunohistochemistry.

Immunohistochemistry protocols. Flat sheets (1 cm × 0.5 cm) from small bowel and colon were used. Tissues were fixed in 4% PFA-PB for 4 h separately, then washed in PBS, and moved into 30% sucrose in PBS overnight and then frozen in OCT embedding compound (Sakura Finetek) at −80 °C until sectioned. Tissues were cut into 12-μm-thick sections, rinsed with PBS twice for 5 min, and blocked with 200 μL per slide of 1% BSA/PBS/0.3% Triton X/10% normal donkey serum in a humidity chamber. Primary antibodies (*SI Appendix*, Table S2) were added in 200 μL per slide of BSA/PBS/0.3% Triton/10% normal donkey serum and were incubated at 4 °C overnight in humidity chamber. Slides were then rinsed five times for 3 min in PBS. Secondary antibody (*SI Appendix*, Table S2) was incubated for 1 h in the dark. Slides were mounted in slowfade gold with DAPI (Life Technologies) mounting buffer.

Colocalization of Piezo2 and EC cells. Imaging was done using BX51W1 epifluorescence (40×, 0.75 NA objective) and FV1000 confocal (60×, 1.2 NA or a 20×, 0.95 NA objectives) microscopes (Olympus). Epithelial CFP^+ and/or $Piezo2^+$ cells were defined by DAPI-staining as the luminal facing layer of the mucosa. CFP^+ cells and $Piezo2^+$ cells were counted separately. Area-proportional Venn diagrams were graphed with BioVenn software (biovenn.nl).

SIM. We used an Elyra PS.1 Super Resolution microscope (Carl Zeiss Microscopy, LLC) with a 63×, 1.4 NA oil-immersion objective, with a 1.5× tube multiplier. Laser-excitation wavelengths were 405, 488, 561, and 642 nm. The *z*-sections ranged from 8 to 10 μm, with slice thickness of 175 nm. A four-image average was used for each *z*-slice of each of the five rotations of the grid. Channels were acquired sequentially, beginning with the 642-nm excitation and ending with 405 nm. ZEN deconvolution software for SIM was used with default settings.

Single-Cell Electrophysiology.

Solutions. The extracellular solution contained: 150 mM Na^+, 5 mM K^+, 2.5 mM Ca^{2+}, 1 mM Mg^{2+},160 mM Cl^-, 5 mM Hepes, and 5.5 mM glucose, pH 7.35, 300 mmol/kg; the intracellular solution contained: 140 mM Cs^+, 150 mM Cl^-, 4 mM Mg^{2+}, 2 mM Ca^{2+}, 10 mM Hepes, and 5 mM EGTA, pH 7.3, 300 mmol/kg.

Data acquisition. Standard whole-cell voltage clamp and mechanical stimulation by a piezoelectric-driven glass probe were used as described previously (11, 21). Electrodes (Kimble KG12 glass) were pulled by Sutter P97 puller (Sutter Instruments), coated with R6101 (Dow Corning), and fire-polished to 2–5 MΩ. Stimulation and data acquisition were done with an Axopatch 200B patch-clamp amplifier, CyberAmp 320 signal conditioner, Digidata 1550A, and pClamp 10.5 software (Molecular Devices). Whole-cell voltage-clamp signals were sampled at 20 kHz and filtered at 4 kHz. Series resistance was compensated in all whole-cell recordings. Cells held at −120 mV, and voltage-dependent currents were recorded from −80 through +15 mV in 5-mV steps for 50 ms to measure steady-state activation, then stepped to 0 mV for 50 ms to measure steady-state inactivation. The start-to-start time was 250 ms per sweep and 6 s per run for up to 10 runs. Mechanical stimulation was applied as stated in results via fire-polished glass microelectrodes driven by a piezotransducer P-621.1CD attached to an E-625.CR controller (Physik Instrumente). Displacement ladders were 50-ms steps of 0.3-μm increments at a 0.6-μm/ms upstroke/downstroke rate.

Data analysis. Whole-cell patch-clamp data were analyzed in pClamp 10.5 (Molecular Devices). The peak currents within 10 ms of stimulus start were selected for analysis. pClamp (Molecular Devices) and Origin 2016 (OriginLab Co.) were used for electrophysiology data analysis. Current–voltage relationships were fit with a linear function, $V = A + B \times I$, where the parameters were: I current, V voltage, A y-intercept, and B the slope. Displacement-current curves were fit using a Boltzmann function $I = A2 + (A1 - A2)/(1 + exp((x - x0)/dx))$, where the parameters were: I current, $A1$ y-intercept, $A2$ peak, x displacement, $x0$ half-point displacement, dx slope displacement.

For whole-cell recording experiments significance was assigned when $P < 0.05$ by Student t tests, as specified in the text, and specifically two-tailed unpaired t tests with Welch's correction (Control vs. treatment) (Fig. 3) using GraphPad Prism v6 (GraphPad Software, https://www.graphpad.com/).

Calcium Imaging. Primary cultures from *NeuroD1-cre;GCaMP5-tdTomato* mice were dissociated and grown for 24 h in MatTek dishes (MatTek Corporation) as above. Bath solution contained: 150 mM NaCl, 5 mM KCl, 2 mM $MgCl_2$, 2 mM $CaCl_2$, 10 mM glucose, and 10 mM Hepes, pH 7.3, 320 mmol/kg (adjusted with sucrose) and viscosity 0.0077 P. Cultures were placed on an inverted Olympus IX70 epifluorescence microscope (Olympus) and imaged with a 16-bit high-speed camera (Hamamatsu). Cells were continuously perfused with bath solution (10 mL/min) and shear force was applied using 500-μm manifold (ALA Scientific Instruments) controlled by Octaflow (ALA Scientific Instruments). Flow rate (microliter per second, μL/s) depended on applied pressure (PSI) and manifold radius. Shear force was calculated using the equation: $S = 4\mu Q/(\pi r^3)$, where μ is fluid viscosity of the bath solution (0.0077 Pa) (54), Q is the flow rate (μL/s), and πr^3 is the volume of the manifold (r = 250 μm). Using pressures from 1 to 20 PSI, the applied shear force ranged from 0.04 to 2.0 dyn/cm^2. EC cells were identified by TdTomato fluorescence. GCaMP5 was excited at 480/505 nm and fluorescence emission was collected at 525 nm. Images were taken using the 40× objective and acquired at three frames per second (100-ms exposure time/frame) with Metamorph Software (Molecular Devices). Cells were stimulated either with shear force or high KCl (50 mM), with 15- to 30-min intervals of recovery

unless otherwise indicated. Blockers were preapplied through the bath and coapplied during shear. Ca^{2+}-free bath solution, Gd^{3+} (30 μM), D-GsMTx4 (10 μM), and AITC (150 μM) solutions were freshly prepared on the day of the experiments. All experiments were performed at room temperature (25 °C). Fluorescence time series were converted to $\Delta F/F_0$ ($\Delta F/F_0 = (F - F_0)/F_0$), where F_0 is the baseline fluorescence for each trial.

5-HT Biosensor Experiments. High-conductance nondesensitizing 5-HT_3R was a kind gift of Cecilia Bouzat, Instituto de Investigaciones Bioquímicas de Bahía Blanca, CONICET Bahía Blanca, Argentina (32). HEK293 cells were cotransfected with 5-HT_3R and GCaMP5G (1 μg/μL; Addgene #31788) and cocultured with primary EC cells for 24 h before the experiments. Primary EC cells were mechanically stimulated using a fire-polished glass microelectrode (3.0-μm indentation, 50-ms duration) driven by a piezotransducer P-621.1CD attached to an E-625.CR controller (Physik Instrumente). D-GsMTx4 (10 μM), 5-HT (1–10 μM), ondansetron (0.1 μM), Yoda1 (10 μM), and AITC (150 μM) were freshly made on the day of the experiments. Acquisition and experimental conditions were as described in the previous section.

Üssing Chamber.

Solutions. The Krebs-Ringer solution consisted of: 120 mM NaCl, 5.9 mM KCl, 15 mM NaH_2CO_3, 1.6 mM NaH_2PO_4, 1.3 mM $CaCl_2$, 2.4 mM $MgCl_2$, pH = 7.4, gassed with 95/5 mixture of O_2/CO_2. Glucose (10 mM) was added to the serosa bath and mannitol (10 mM) was added to the mucosa bath to maintain osmotic balance.

Tissue preparation. Segments of jejunum (4 cm) were cut along the mesenteric border, and luminal contents were gently removed. Tissue was cut into 2-cm segments. During preparation, the tissues were bathed in ice-cold Krebs-Ringer solution.

Short-circuit current measurements with mechanical pressure. The full-thickness preparations of mouse jejunum with a cross-sectional area of 0.3 cm^2 were mounted in 4-mL Üssing chambers (Physiologic Instruments). Transepithelial potential difference was measured using paired Ag-AgCl electrodes via 3% Agar with 3-M KCl bridges and clamped at 0 mV by another pair of Ag-AgCl electrodes. The mucosal and serosal surfaces of the tissue were bathed with 4 mL of Krebs-Ringer solution with mannitol and glucose, respectively, maintained at 37 °C during the experiments. Tissue equilibrated to attain stable basal short-circuit current (I_{sc}) and tissue conductance (G_t) for 30 min before conducting the experiment. Hydrostatic pressure was applied using DPM-1 pneumatic transducer (Bio-Tek Instruments) in a sealed mucosal chamber. Pressure stimuli of 10-s duration were applied from rest (atmospheric pressure). To assure tissue viability, acetylcholine (100 μM) was applied to the serosal side at the end of the experiment. Tissue was not used if there was no response to acetylcholine. Data were recorded using Acquire and Analyze 2.3 (Physiologic Instruments).

Data analysis. Raw data were exported into text format and uploaded into Clampfit 10.5 (Molecular Devices). Pressure-induced peak short-circuit current (I_{sc}) was measured $\Delta I_{sc} = I_{sc\_peak} - I_{sc\_baseline}$. Statistical significance was assigned for $P < 0.05$ (*) using an unpaired two-tailed t test.

ACKNOWLEDGMENTS. We thank Mrs. Lyndsay Busby for administrative assistance, and Mr. Eugene Kruger and the Mayo Clinic Optical Core for assistance with confocal imaging of organoids. This work was supported by Grant NIH DK106456, Pilot and Feasibility Grant from the Mayo Clinic Center for Cell Signaling in Gastroenterology (NIH DK084567), and a 2015 American Gastroenterological Association Research Scholar Award (AGA RSA) (all to A.B.); NIH Grants DK100223 and DK110614 (to A.B.L.); and NIH Grant DK052766 (to G.F.).

1. Bulbring E, Crema A (1959) The release of 5-hydroxytryptamine in relation to pressure exerted on the intestinal mucosa. *J Physiol* 146:18–28.
2. Bertrand PP (2004) Real-time detection of serotonin release from enterochromaffin cells of the guinea-pig ileum. *Neurogastroenterol Motil* 16:511–514.
3. Sidhu M, Cooke HJ (1995) Role for 5-HT and ACh in submucosal reflexes mediating colonic secretion. *Am J Physiol* 269:G346–G351.
4. Cooke HJ, Sidhu M, Wang YZ (1997) 5-HT activates neural reflexes regulating secretion in the guinea-pig colon. *Neurogastroenterol Motil* 9:181–186.
5. Heredia DJ, Dickson EJ, Bayguinov PO, Hennig GW, Smith TK (2009) Localized release of serotonin (5-hydroxytryptamine) by a fecal pellet regulates migrating motor complexes in murine colon. *Gastroenterology* 136:1328–1338.
6. Erspamer V (1957) Occurrence and distribution of 5-hydroxytryptamine (enteramine) in the living organism. *Z Vitam Horm Fermentforsch* 9:74–96.
7. Côté F, et al. (2003) Disruption of the nonneuronal tph1 gene demonstrates the importance of peripheral serotonin in cardiac function. *Proc Natl Acad Sci USA* 100: 13525–13530.
8. Bulbring E, Crema A (1958) Observations concerning the action of 5-hydroxytryptamine on the peristaltic reflex. *Br J Pharmacol Chemother* 13:444–457.
9. Chin A, et al. (2012) The role of mechanical forces and adenosine in the regulation of intestinal enterochromaffin cell serotonin secretion. *Am J Physiol Gastrointest Liver Physiol* 302:G397–G405.
10. Kim M, Javed NH, Yu JG, Christofi F, Cooke HJ (2001) Mechanical stimulation activates Galphaq signaling pathways and 5-hydroxytryptamine release from human carcinoid BON cells. *J Clin Invest* 108:1051–1059.
11. Wang F, et al. (2017) Mechanosensitive ion channel Piezo2 is important for enterochromaffin cell response to mechanical forces. *J Physiol* 595:79–91.
12. Ikeda R, Gu JG (2014) Piezo2 channel conductance and localization domains in Merkel cells of rat whisker hair follicles. *Neurosci Lett* 583:210–215.
13. Woo SH, et al. (2014) Piezo2 is required for Merkel-cell mechanotransduction. *Nature* 509:622–626.
14. Chang W, et al. (2016) Merkel disc is a serotonergic synapse in the epidermis for transmitting tactile signals in mammals. *Proc Natl Acad Sci USA* 113:E5491–E5500.
15. Li HJ, et al. (2014) Distinct cellular origins for serotonin-expressing and enterochromaffin-like cells in the gastric corpus. *Gastroenterology* 146:754–764.e3.
16. Sjölund K, Sandén G, Håkanson R, Sundler F (1983) Endocrine cells in human intestine: An immunocytochemical study. *Gastroenterology* 85:1120–1130.
17. Fothergill LJ, Callaghan B, Hunne B, Bravo DM, Furness JB (2017) Costorage of enteroendocrine hormones evaluated at the cell and subcellular levels in male mice. *Endocrinology* 158:2113–2123.
18. Haber AL, et al. (2017) A single-cell survey of the small intestinal epithelium. *Nature* 551:333–339.
19. Ray SK, Li HJ, Metzger E, Schüle R, Leiter AB (2014) CtBP and associated LSD1 are required for transcriptional activation by NeuroD1 in gastrointestinal endocrine cells. *Mol Cell Biol* 34:2308–2317.
20. Sanz E, et al. (2009) Cell-type-specific isolation of ribosome-associated mRNA from complex tissues. *Proc Natl Acad Sci USA* 106:13939–13944.
21. Strege PR, et al. (2017) Sodium channel $Na_V1.3$ is important for enterochromaffin cell excitability and serotonin release. *Sci Rep* 7:15650.
22. Knutson K, et al. (2018) Whole cell electrophysiology of primary cultured murine enterochromaffin (EC) cells. *J Vis Exp*, 10.3791/58112.
23. Coste B, et al. (2010) Piezo1 and Piezo2 are essential components of distinct mechanically activated cation channels. *Science* 330:55–60.
24. Alcaino C, Knutson K, Gottlieb PA, Farrugia G, Beyder A (2017) Mechanosensitive ion channel Piezo2 is inhibited by D-GsMTx4. *Channels (Austin)* 11:245–253.
25. Kuwabara T, et al. (2009) Wnt-mediated activation of NeuroD1 and retro-elements during adult neurogenesis. *Nat Neurosci* 12:1097–1105.
26. Hu H, Sachs F (1996) Mechanically activated currents in chick heart cells. *J Membr Biol* 154:205–216.
27. Bae C, Sachs F, Gottlieb PA (2011) The mechanosensitive ion channel Piezo1 is inhibited by the peptide GsMTx4. *Biochemistry* 50:6295–6300.
28. Bellono NW, et al. (2017) Enterochromaffin cells are gut chemosensors that couple to sensory neural pathways. *Cell* 170:185–198.e16.
29. Nozawa K, et al. (2009) TRPA1 regulates gastrointestinal motility through serotonin release from enterochromaffin cells. *Proc Natl Acad Sci USA* 106:3408–3413.
30. Sato T, et al. (2009) Single Lgr5 stem cells build crypt-villus structures in vitro without a mesenchymal niche. *Nature* 459:262–265.
31. Thorne CA, et al. (2018) Enteroid monolayers reveal an autonomous WNT and BMP circuit controlling intestinal epithelial growth and organization. *Dev Cell* 44:624–633.e4.
32. Corradi J, Gumilar F, Bouzat C (2009) Single-channel kinetic analysis for activation and desensitization of homomeric 5-HT(3)A receptors. *Biophys J* 97:1335–1345.
33. Clarke LL (2009) A guide to Ussing chamber studies of mouse intestine. *Am J Physiol Gastrointest Liver Physiol* 296:G1151–G1166.
34. Psichas A, Reimann F, Gribble FM (2015) Gut chemosensing mechanisms. *J Clin Invest* 125:908–917.
35. Bulbring E, Lin RC (1958) The effect of intraluminal application of 5-hydroxytryptamine and 5-hydroxytryptophan on peristalsis; the local production of 5-HT and its release in relation to intraluminal pressure and propulsive activity. *J Physiol* 140:381–407.
36. Grün D, et al. (2015) Single-cell messenger RNA sequencing reveals rare intestinal cell types. *Nature* 525:251–255.
37. Reynaud Y, et al. (2016) The chemical coding of 5-hydroxytryptamine containing enteroendocrine cells in the mouse gastrointestinal tract. *Cell Tissue Res* 364:489–497.
38. Li HJ, Ray SK, Singh NK, Johnston B, Leiter AB (2011) Basic helix-loop-helix transcription factors and enteroendocrine cell differentiation. *Diabetes Obes Metab* 13:5–12.
39. Sumara G, Sumara O, Kim JK, Karsenty G (2012) Gut-derived serotonin is a multifunctional determinant to fasting adaptation. *Cell Metab* 16:588–600.
40. Bertrand PP (2006) Real-time measurement of serotonin release and motility in guinea pig ileum. *J Physiol* 577:689–704.
41. Coste B, et al. (2013) Gain-of-function mutations in the mechanically activated ion channel PIEZO2 cause a subtype of distal arthrogryposis. *Proc Natl Acad Sci USA* 110: 4667–4672.
42. Ikeda R, et al. (2014) Merkel cells transduce and encode tactile stimuli to drive Aβ-afferent impulses. *Cell* 157:664–675.
43. Ranade SS, et al. (2014) Piezo2 is the major transducer of mechanical forces for touch sensation in mice. *Nature* 516:121–125.
44. Woo SH, et al. (2015) Piezo2 is the principal mechanotransduction channel for proprioception. *Nat Neurosci* 18:1756–1762.
45. Kirchgessner AL, Tamir H, Gershon MD (1992) Identification and stimulation by serotonin of intrinsic sensory neurons of the submucosal plexus of the guinea pig gut: Activity-induced expression of Fos immunoreactivity. *J Neurosci* 12: 235–248.

46. Allen TG (1997) The 'sniffer-patch' technique for detection of neurotransmitter release. *Trends Neurosci* 20:192–197.
47. Rogers GJ, et al. (2011) Electrical activity-triggered glucagon-like peptide-1 secretion from primary murine L-cells. *J Physiol* 589:1081–1093.
48. Lomax RB, Gallego S, Novalbos J, García AG, Warhurst G (1999) L-type calcium channels in enterochromaffin cells from guinea pig and human duodenal crypts: An in situ study. *Gastroenterology* 117:1363–1369.
49. Raghupathi R, et al. (2013) Identification of unique release kinetics of serotonin from guinea-pig and human enterochromaffin cells. *J Physiol* 591:5959–5975.
50. Liñán-Rico A, et al. (2017) UTP-gated signaling pathways of 5-HT release from BON cells as a model of human enterochromaffin cells. *Front Pharmacol* 8:429.
51. Liñán-Rico A, et al. (2013) Purinergic autocrine regulation of mechanosensitivity and serotonin release in a human EC model: ATP-gated P2X3 channels in EC are downregulated in ulcerative colitis. *Inflamm Bowel Dis* 19:2366–2379.
52. Pettersson G (1979) The neural control of the serotonin content in mammalian enterochromaffin cells. *Acta Physiol Scand Suppl* 470:1–30.
53. Kunze WA, Clerc N, Furness JB, Gola M (2000) The soma and neurites of primary afferent neurons in the guinea-pig intestine respond differentially to deformation. *J Physiol* 526:375–385.
54. Cha M, Ling J, Xu GY, Gu JG (2011) Shear mechanical force induces an increase of intracellular Ca2+ in cultured Merkel cells prepared from rat vibrissal hair follicles. *J Neurophysiol* 106:460–469.